Albert Polman.

Synthesis and Optical Characterization of Si nano-clusters in an SiO_2 matrix.

M.L. Brongersma.

June 1994.

The experiments described in this report are the result of a nine month graduation project done at the FOM-Institute for Atomic and Molecular Physics (AMOLF) in Amsterdam. (September 1993 - June 1994)

Supervisor at AMOLF. Dr. A. Polman
Supervisor at TUE. Prof. dr. M.J.A. de Voigt

ABSTRACT

Si-rich SiO_2 films were prepared by both ion implantation of Si into SiO_2 (50 keV, $5 \cdot 10^{16}$ Si/cm^2 or 175 keV, $5 \cdot 10^{16}$ Si/cm^2), and by chemical vapour deposition (CVD) from SiH_4 and N_2O. Rutherford backscattering spectrometry data confirms that the ion implanted samples locally contain a few atomic percent excess Si. The CVD grown films consist of 52 at.% Si and 48 at.% O. These films were subsequently annealed at temperatures between 700 °C and 1200 °C to induce precipitation of Si nano-crystals.

The evolution of the nano-structure upon annealing was studied by Raman spectroscopy. The Si implanted SiO_2 films contain too little nano-crystalline Si material to extract information on the nano-structure by Raman spectroscopy. The CVD grown films show a clear amorphous to crystalline transition upon annealing at 1000 °C for 5 minutes. Furthermore, the Raman spectrum after annealing at 1200 °C indicates the presence of Si crystallites with characteristic dimensions of ≤ 9 nm.

After annealing at 700 °C for 40 minutes the implanted films show clear room temperature luminescence, attributed to band-to-band transitions in Si nano-crystals. The luminescence peaks around roughly 0.7 µm, corresponding to a cluster size of typically 4 nm. A red-shift is observed upon annealing at 1000 °C, attributed to an increase in the average cluster size by Ostwald ripening. Comparing the 50 keV and 175 keV implants it is concluded that smaller clusters have formed when the Si supersaturation is less. Infrared luminescence in the range of 1.14 - 1.5 µm is also observed and is attributed to interface states at the Si/SiO_2 interface or defect states in the Si nano-crystals, indicating that the quantum efficiency for band-to-band recombination in the nano-crystals is less than 100 %. No luminescence from the CVD grown samples was observed, indicating that quantum confinement effects are not efficient when the Si cluster volume fraction is as large as 31%.

CONTENTS

Abstract.

I.	**Introduction.**	1
II.	**Experimental.**	3
III.	**Sample preparation.**	4
IV.	**Compositional analysis using Rutherford backscattering spectrometry.**	5
V.	**Raman spectroscopy of Si nano-crystals.**	6
VI.	**Photoluminescence spectroscopy (0.5-1.1 μm) of Si implanted SiO_2 films and SIPOS.**	8
	A. Excess Si or defect luminescence: Si versus Ne implants in SiO_2.	8
	B. PL versus anneal temperature and implantation energy.	9
	C. PL spectroscopy on SIPOS.	11
VII.	**Photoluminescence spectroscopy (1.0-1.6 μm) of Si implanted SiO_2 films.**	12
VIII.	Conclusions.	13
IX.	Technological assessment.	14
	References.	15
	Appendix I: Sensitivity curves from the PMT and Ge detector.	16
	Acknowledgements.	17

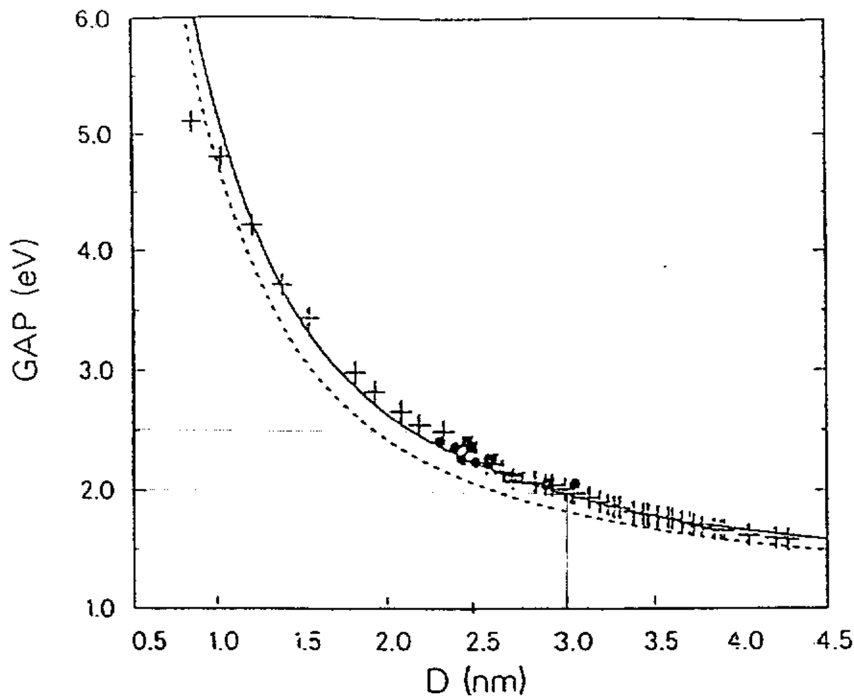

FIG.1. Calculated optical bandgap energies for various Si crystallites as a function of diameter (drawn lines). The black dots are the experimental results from ref. 3 in which Si nano-crystals were synthesized using a reactive sputtering technique.

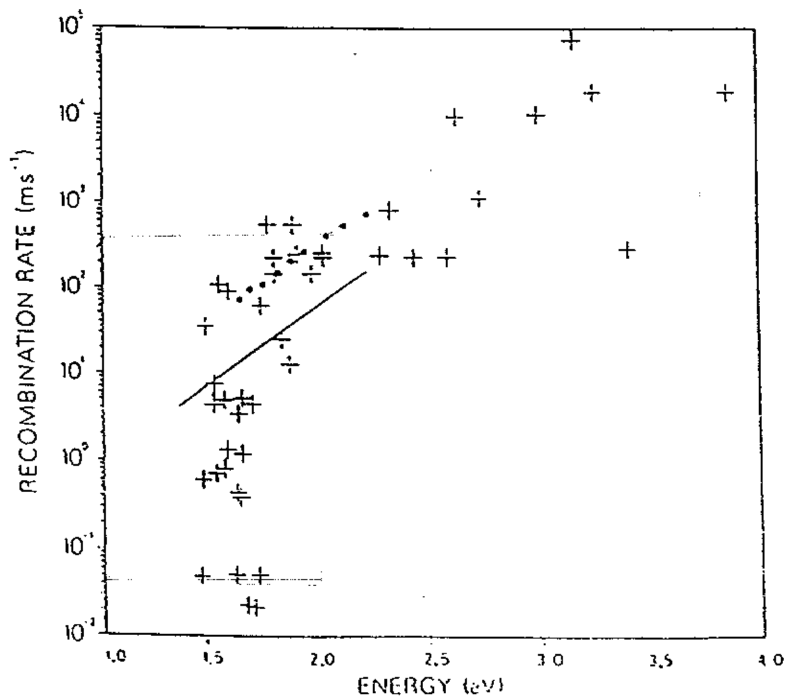

FIG.2. Electron-hole recombination rate as a function of the bandgap energy, as calculated in Ref.2.

I. INTRODUCTION.

Although Si is the key element in todays' semiconductor industry it never made it in the world of optoelectronics. This can be attributed to the fact that Si, due to its indirect band gap, shows very inefficient radiative band-to-band recombination. Several methods have been applied to circumvent this problem. For example, rare-earth doping with, for instance, Er is employed with the aim to electrically induce internal optical transitions in the Er ion. Another possible approach is based on the fact that the Si bandstructure can be tailored through alloying Si with elements such as Ge. Also, it was recently found that porous Si, fabricated by electrochemical anodization of single crystalline Si, shows very strong visible luminescence at room temperature [1].

This luminescence is believed to arise from quantum confinement in the nano-crystalline Si structures which increases the band gap as well as the recombination rate corresponding to the optical transition across the gap [2,3,4]. This is illustrated in Fig. 1, taken from ref. 2, which shows a calculation of the optical bandgap of Si crystallites as a function of diameter. The figure shows significant deviation from the bulk Si bandgap (1.1 eV) for clusters of nm size. In Fig. 2, which was also taken from ref. 2, a calculation of the recombination rate as a function of the bandgap is plotted. The recombination rate exhibits a strong dependence on the bandgap energy and thus implicitly on cluster size. At first, this quantum confinement model was questioned, as the light emission from porous Si could also be attributed to silicon based compounds, such as siloxene ($Si_6O_3H_6$) [5], which are present at the surface of the nano-crystallites. However, most evidence now points in favour of models based on the quantum confinement effect [6,7].

One problem in the study of porous Si is that it is very difficult to characterize the irregular structure of the material. This makes the investigation of the relation between nano-structure and its optical properties nearly impossible. It is, therefore, desirable to find systems in which the nano-crystalline structures can be made in a much more controlled way. For example, SiO_2 is an ideal host material for Si nano-crystals. It is an easily grown, well-defined material and allows for good passivation of surface states. It is known that nano-crystals with a very well-defined structure and cluster size distribution can be grown by annealing a supersaturated solid solution of Si in SiO_2 [8,9]

In the following, it will be shown how ion implantation and chemical vapour

deposition can be used for synthesizing Si nano-crystals in a SiO_2 matrix. The use of ion implantation for this purpose is a new approach, although another group has also recently adopted this idea [10]. Rutherford backscattering, Raman spectroscopy and photoluminescence measurements in the visible as well as in the infrared were performed to gain insight in the structural and optical properties of these samples.

II. EXPERIMENTAL.

Ion implantation of Si into SiO_2 was performed with a single ended 1 MV Van de Graaff-type accelerator. SiF_4 gas was fed into a cold cathode Penning source to produce a $^{28}Si^+$ ion beam. Prior to acceleration, a coarse mass separation was made in a Wien filter to prevent unwanted ions from acceleration. After acceleration, the beam passed through an electrostatic quadrupole lens and an analyzing magnet. A Si current of typically 2 $\mu A/cm^2$ was obtained on target. The ion beam was electrostatically scanned through a 1.5×1.5 cm^2 aperture to obtain a uniform implant. All samples were kept at room temperature during implantation.

Rutherford backscattering spectrometry measurements were made with a single-ended 2 MV Van de Graaff-type accelerator that can deliver a He^+ current on the target of over 100 nA with an angular spread of less than 0.1 °. Backscattered He^+ ions were detected using a standard Si surface barrier detector, which was cooled to 0 °C to obtain an energy resolution of about 15 keV FWHM (full width at half maximum). Spectra were taken in random as well as channeling directions using 2 MeV He ions and a scattering angle of either 168° or 105° depending on the experiment. A more detailed description of the MeV facilities has been published elsewhere [11].

Raman spectra were measured using the 514.5 nm line of an Ar-ion laser with a power of 100 mW as a light source. Spectra were taken in a quasi-backscattering geometry with an incident angle of about 30° with the sample normal. Measurements were done with a resolution of 1.8 cm^{-1}.

Photoluminescence (PL) measurements in the spectral range of 0.5 μm to 1.1 μm were performed with the 488 nm line of an Ar-ion laser as an excitation source. The visible luminescence was dispersed by a 48 cm monochromator and then imaged onto a photomultiplier tube (PMT). In the spectral range of 0.9 μm to 1.7 μm the 514 nm laser line of the Ar-ion laser was employed as excitation source and a liquid-nitrogen cooled Ge detector was used for the detection of the luminescence signal. In all cases the laser beam was modulated using a mechanical chopper and the signals from the detector were recorded using a lock-in amplifier using the chopper signal as a reference. Pump powers used in the experiments were typically 100 mW and the spectral resolution of the monochromator was set typically at 6 nm. Some measurements were performed with samples cooled to 77 K using a closed-cycle He refrigerator cryostat. All PL spectra have been corrected for the sensitivities of the PMT and Ge detector (see appendix I).

III. SAMPLE PREPARATION.

Two different techniques have been used to obtain Si nano-crystals in an SiO_2 matrix. Supersaturated solid solutions were first created by ion implantation of Si into SiO_2, or by chemical vapour deposition. These samples were then annealed with the aim to nucleate small Si clusters. Nucleation is a process determined by a competition between volume and surface energies. The final cluster size distribution will depend on the annealing temperature as well as the degree of supersaturation.

The advantage of ion implantation is that this technique provides for a way to produce a well defined concentration depth profile of Si particles in the host material. SiO_2 films with thicknesses of 180 nm and 800 nm were grown by thermal oxidation at 1000 °C of Si (100) substrates. The 180 nm thick films were implanted with 50 keV Si, the 800 nm thick films with 175 keV Si, both at a fluence of $5\cdot10^{16}$ Si/cm^2. For both cases the Si projected range was within the SiO_2 film. The samples were subsequently annealed at a temperature of 700 °C for 40 min in a tube furnace with a pressure below 10^{-6} Torr. Some of the samples received an additional anneal at a temperature of 1000 °C for either 1 hour or 12 hours.

A second set of samples was made by low pressure chemical vapour deposition (LPCVD) of SiH_4 and N_2O. The stoichiometry of the resulting SiO_x films can be varied between x=0 (pure Si) and x=2 (SiO_2) by varying the gas-flow rates. For these experiments films were deposited on Si(100) substrates at a temperature of 620°C and an ambient pressure of 400 mTorr. The films were deposited with a thickness of about 420 nm and a Si concentration of 52 at.%. The as-deposited films were annealed in a rapid thermal annealer with a N_2 ambient for 5 minutes at 800 °C, 1000 °C and at 1200 °C. Transmission electron microscopy (TEM) shows that the as-deposited films are amorphous. Since Si and O atoms are randomly distributed during deposition, the precipitation process is different from that in the Si implanted SiO_2 samples. A large amount of potential nano-cluster material with a high degree of supersaturation can easily be obtained using this fabrication method. In the semiconductor industry these films, known as semi-insulating polycrystalline silicon (SIPOS), are used as passivating material in Si-based electronic devices.

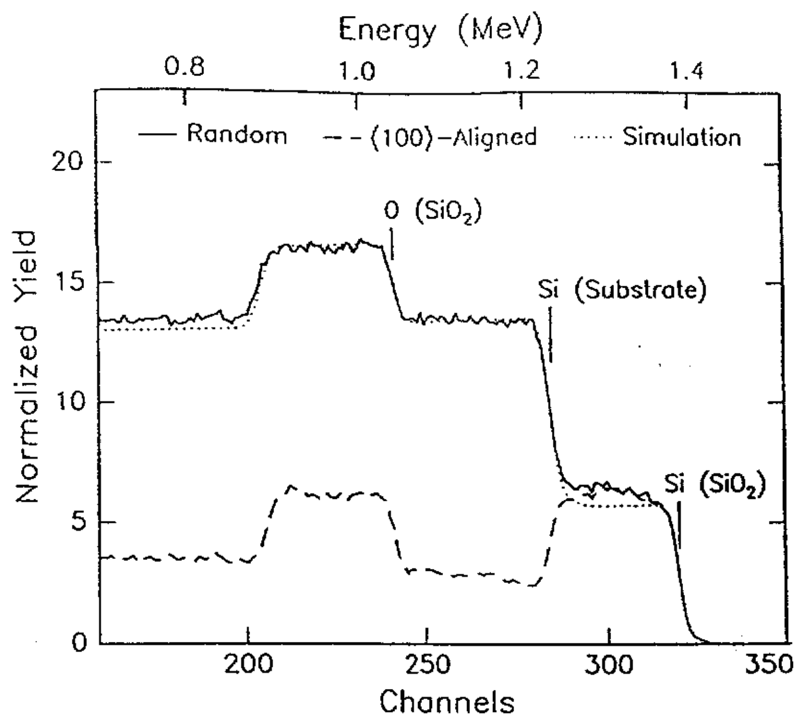

FIG.3. RBS/channeling spectra for the $5 \cdot 10^{16}$ /cm^2 50 keV Si implanted SiO_2 film on a Si (100) substrate taken at a scattering angle of 168°. The RUMP simulation of a 140 nm thick SiO_2 film on top of a Si substrate is also shown. The local enrichment of the SiO_2 film with a few atomic percent Si, can easily be seen in the Si part of the spectrum from SiO_2.

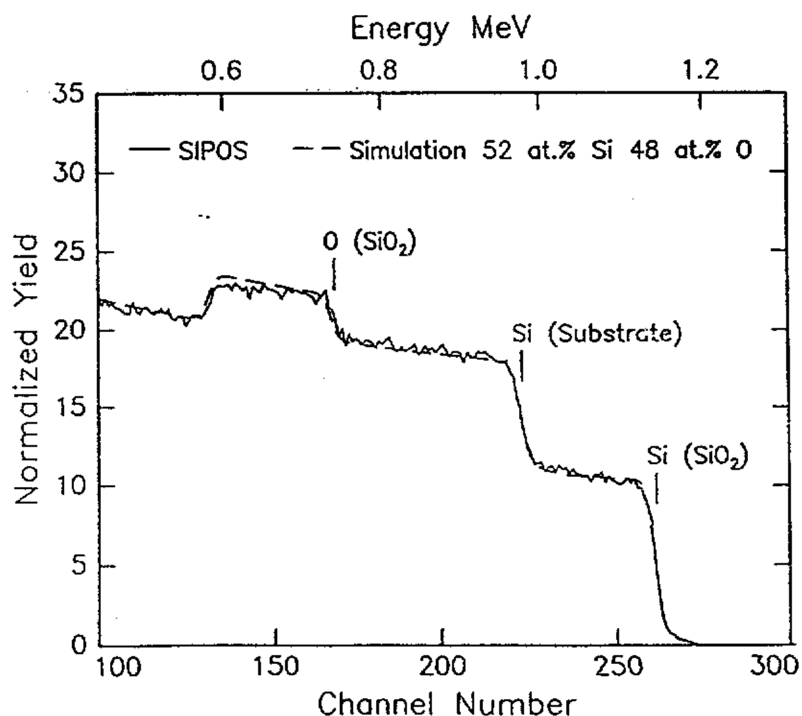

FIG.4. RBS spectrum obtained from the as-deposited SIPOS film on a Si (100) substrate taken at a scattering angle of 105°. A RUMP simulation of a 420 nm thick SIPOS film consisting of 52 at.% Si and 48 at.% O is also shown.

IV. COMPOSITIONAL ANALYSIS USING RUTHERFORD BACKSCATTERING SPECTROMETRY.

Rutherford backscattering spectrometry (RBS) was used to quantify the degree of excess Si in both the Si implanted SiO_2 films as well as the SIPOS films.

Figure 3 shows the RBS/channeling spectra for a SiO_2 film on a Si substrate, implanted with $5 \cdot 10^{16}$ Si/cm^2 at an energy of 50 keV and annealed at 700 °C for 40 minutes. The leading edges of Si- and O in the SiO_2 film as well as the edge from the Si substrate are indicated in the figure. The dashed line represents a RUMP [11] simulation of a 140 nm thick SiO_2 film on top of a Si substrate. The local enrichment of the SiO_2 film with 3 ± 1 at.% Si, can easily be seen in the Si part of the spectrum from the SiO_2. The channeling spectrum shows a reduced yield in the region corresponding to the Si substrate.

The RBS spectrum taken from the as-deposited SIPOS film on a Si(100) substrate, is shown in Fig. 4. The leading edges of Si- and O in the SiO_2 film as well the edge due to the Si substrate have again been indicated in the figure. The dashed line represents a RUMP simulation of a 420 nm thick SIPOS film consisting of 52 at.% Si and 48 at.% O. The Si supersaturation is thus much larger than for the Si implanted SiO_2 films.

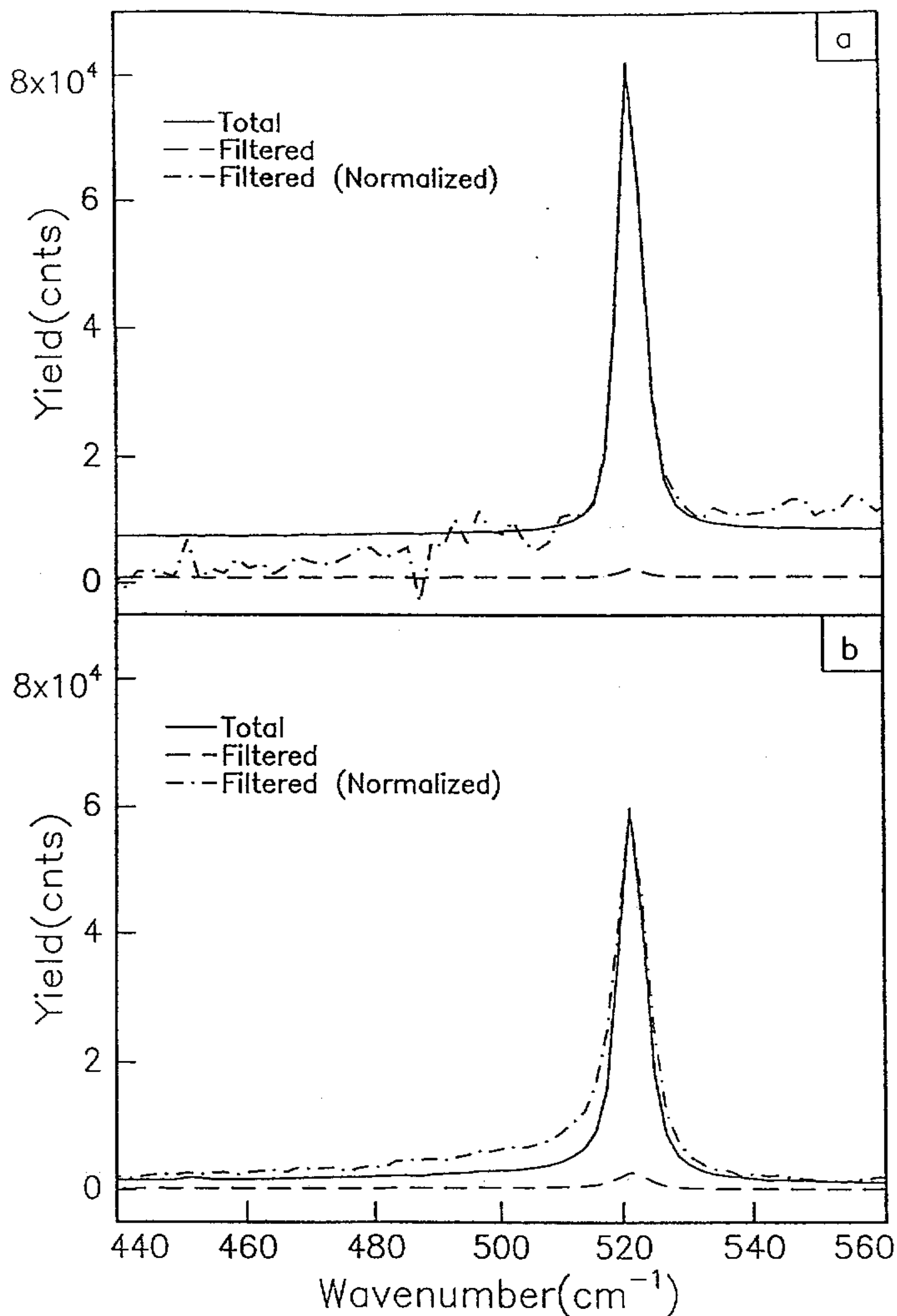

FIG.5 (a) Raman spectra obtained from the sample implanted with $5 \cdot 10^{16}$ Si/cm^2 at 50 keV after annealing at 700 °C for 40 minutes. Spectra of both the total as well as the filtered Raman yield are shown. The sharp symmetric peak at 521 cm^{-1} correspond to the zone-centre TO phonon of crystalline Si.

(b) Raman spectra for the SIPOS film annealed 1200 °C for 5 minutes. Spectra of both the filtered as well as the total Raman yield are shown.

V. RAMAN SPECTROSCOPY OF Si NANO-CRYSTALLITES.

Raman spectroscopy has been demonstrated to be a fast and non-destructive technique which is ideally suited for the characterization of nano-crystalline Si (nc-Si) [13-15]. In this chapter it is shown that by using Raman spectroscopy quantitative information on the crystallinity and size of Si clusters in a SiO_2 matrix can be obtained. Measurements are presented on both the Si implanted SiO_2 films and on the SIPOS films. In both cases the films are grown on a Si substrate. For this reason the substrate contribution to the Raman signal will generally dominate the spectrum. By placing polarization filters in the in- and outgoing beams the contribution from the crystalline substrate can be greatly reduced. However, a small contribution could never be avoided in the present setup.

The Raman spectrum obtained from a Si implanted SiO_2 film is shown in Fig. 5(a) for the sample implanted with $5 \cdot 10^{16}$ Si/cm^2 at 50 keV after annealing at 700 °C for 40 minutes. Spectra are shown of the total and the filtered Raman yield. The sharp symmetric peak centred at 521 cm^{-1} corresponds to the zone-centre TO phonon of c-Si. Because crystal momentum must be conserved in c-Si this is the only peak appearing in the first-order Raman spectrum. The filtered spectrum has a much lower intensity, indicating that the total spectrum is dominated by the substrate. The filtered spectrum will be due to a small remaining contribution of the substrate and possibly a contribution of randomly oriented Si nano-crystallites in the SiO_2 film.

Localization of long wavelength TO phonons in Si nano-crystallites should result in an asymmetric broadening of the first-order Raman line relative to that of the bulk crystalline material [17]. In an attempt to see this subtle effect, the filtered spectrum has been enlarged so that it can be compared with the spectrum from the substrate. No significant broadening of the TO peak is observed. From this it can be concluded that either there is not enough nano-crystalline material present to be detected by Raman spectroscopy, or that the clusters in these samples are so large that phonon confinement effects cannot be observed. Note that Si areal density implanted in these samples ($5 \cdot 10^{16}$ Si/cm^2) corresponds to a thickness of 0.01 μm, much less than the penetration depth of 514 nm light in bulk Si (1 μm), so that only a small contribution to the signal from the clusters is expected.

In Fig. 6 the Raman spectra are shown of as-deposited SIPOS before and after annealing at temperatures of 800 °C, 1000 °C or 1200 °C for 5 minutes. The spectra were taken by filtering the substrate signal, as described above. The spectrum of as-deposited SIPOS is very similar to that of amorphous Si (a-Si) [15]. It is composed of 4 broad

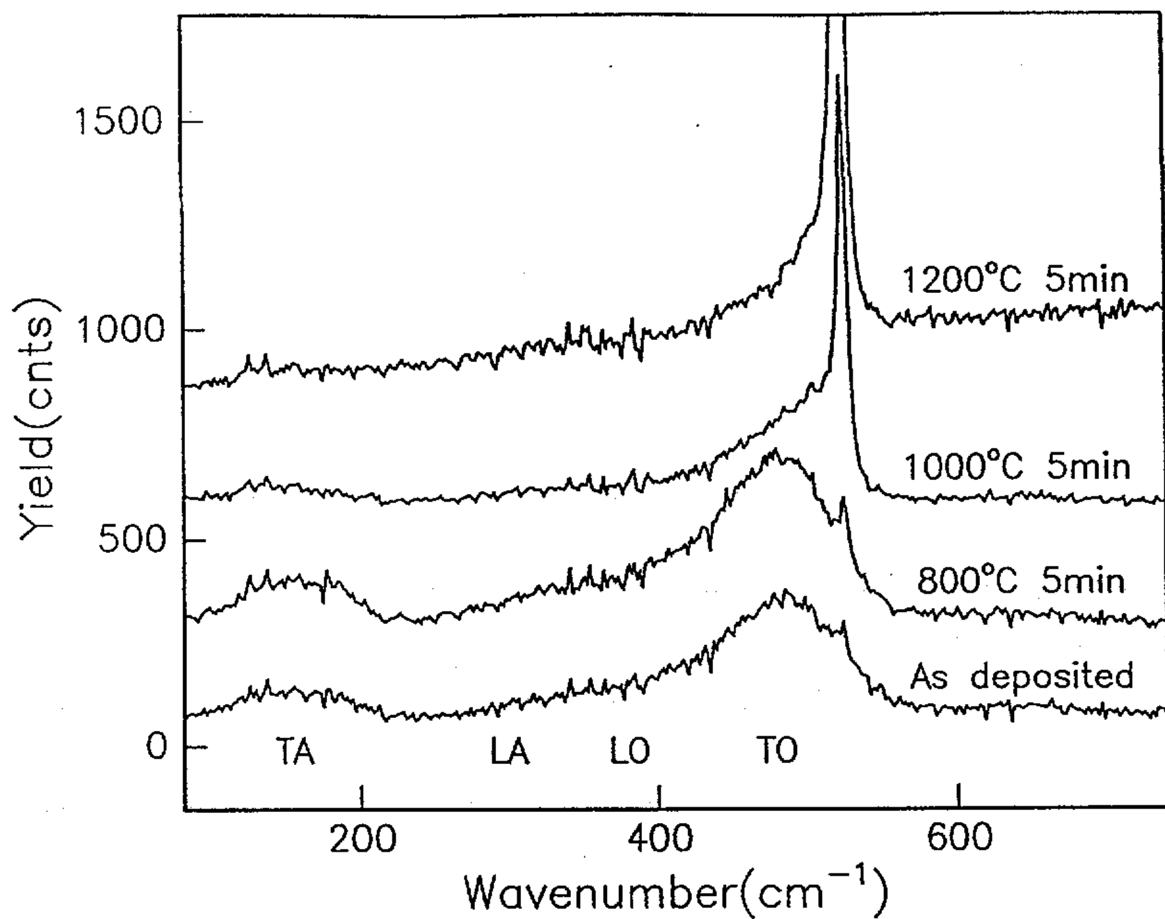

FIG.6. Raman spectra for the as-deposited SIPOS sample before and after annealing at temperatures of 800 °C, 1000 °C and 1200 °C for 5 minutes. A clear transition from amorphous to crystalline can be observed upon annealing.

overlapping bands, corresponding to the transverse acoustic (TA), longitudinal acoustic (LA), longitudinal optic (LO) and transverse optic (TO) peaks. The small sharp peak located at 521 cm^{-1} in the as-deposited SIPOS spectrum is very likely to be due to the underlying Si substrate. However, this peak might also be due to Si crystallites that have formed in the deposition process.

After annealing at 800 °C for 5 minutes, the overall shape of the spectrum does not change much. However, all features grow in intensity. This indicates that some structural rearrangement or relaxation of Si and SiO_2 is taking place, while crystallization is still absent. For example, some phase separation of Si and O may have taken place, with the Si-rich regions still being amorphous.

The spectrum of SIPOS annealed at 1000 °C for 5 minutes shows a sharp TO peak centred at 521 cm^{-1} and resembles the Raman spectrum of c-Si. The characteristic a-Si features have sharply decreased in intensity.

After annealing SIPOS at 1200 °C for 5 minutes the TO peak has sharpened up and the yield has increased even further in comparison to the 1000 °C anneal (the height of the peak which is out of scale amounts to 4200 counts). The TA peak, characteristic of the a-Si spectrum, has vanished completely

From this figure it can be concluded that the amorphous to crystalline transition in SIPOS with a Si:O ratio of 1:1 takes place upon annealing at 1000 °C for 5 minutes. This temperature is high compared to a typical temperature of ~ 700 ° at which homogeneous nucleation of crystalline Si takes place in pure amorphous Si. This can be explained by the fact that, while O increases the nucleation rate, it causes a significant retardation of the epitaxial growth rate. For example, the presence of 1 at.% O decreases the crystallization rate at 650 °C by a factor 17 [17].

Fig. 5(b) shows a detail of the Raman spectrum obtained from SIPOS annealed at 1200 °C for 5 minutes. Just as in Fig. 5(a), the spectra of the total as well as the filtered Raman yield are shown. Again use of polarization filters proves to be a very effective means for reducing the substrate contribution. After enlarging the filtered spectrum a broad asymmetric tail is clearly visible at the low wavenumber side. Since the contribution from the a-Si spectrum to the TO peak is expected to be negligible for this anneal treatment, broadening can only be attributed to the presence of nano-crystalline Si. Using a model that correlates the average crystallite size to the FWHM of the TO peak [16], we estimate an upper limit of average cluster size of about 9 nm in this sample. This is in agreement with TEM observations.

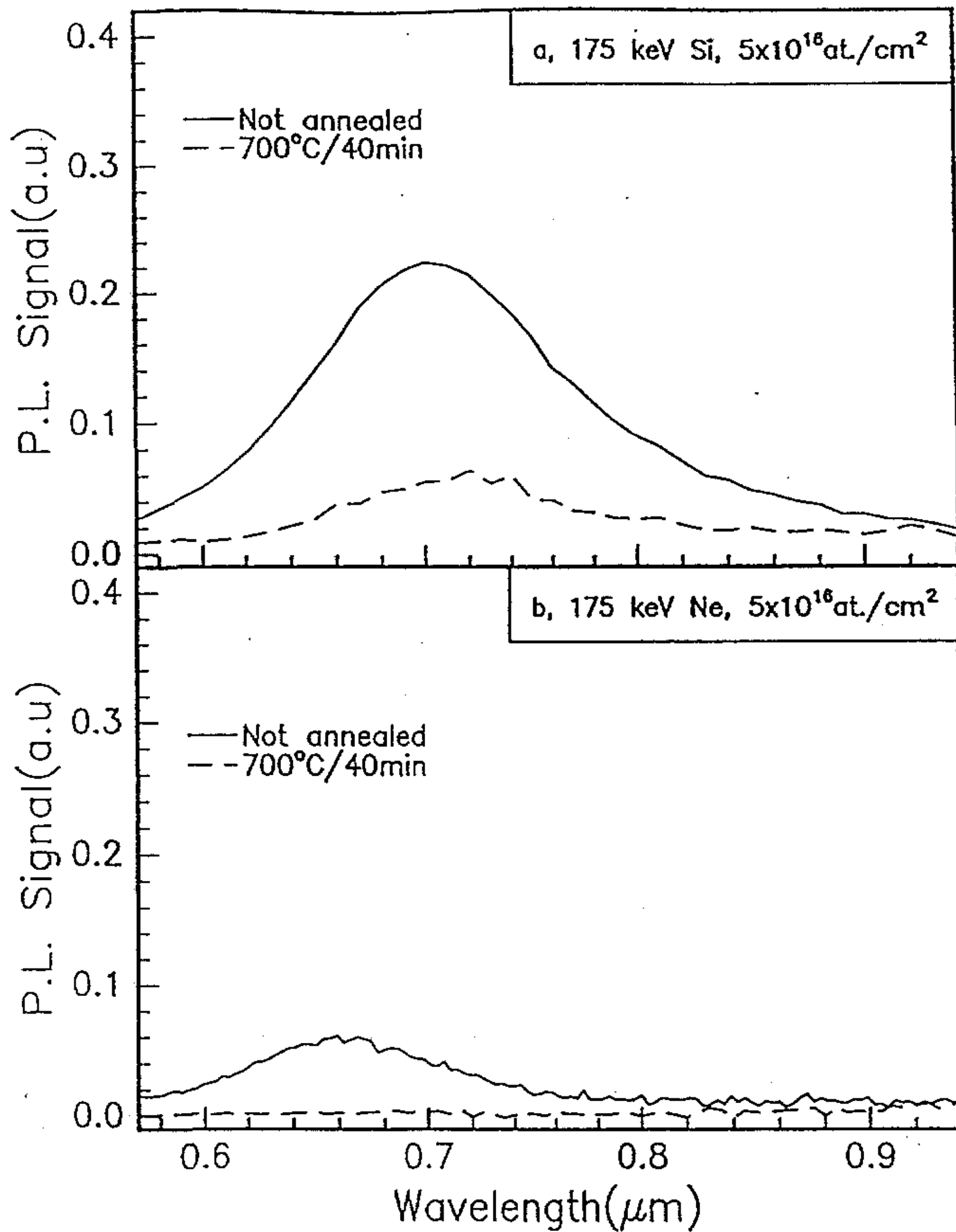

FIG.7 (a) Room temperature photoluminescence spectra for $5\cdot10^{16}$ /cm^2 175 keV Si implanted SiO_2 films before and after annealing at 700 °C for 40 minutes. A 488 nm excitation source was used; The spectral resolution was 6 nm.

(b) Same as (a) but now for 175 keV Ne implanted SiO_2 films.

VI. PHOTOLUMINESCENCE SPECTROSCOPY (0.5-1.1 μm) Of Si IMPLANTED SiO_2 FILMS AND SIPOS.

Photoluminescence (PL) spectroscopy has extensively been used to study the optical properties of Si. We have employed this technique to investigate the luminescence from the Si implanted SiO_2 films and SIPOS samples. Since ion implantation is well-known for creating luminescence centers in SiO_2 [18], the possibility of ion induced defect luminescence was checked (VI.A) by comparing Si and Ne implants. Furthermore, PL spectra taken from the Si implanted SiO_2 films are correlated with anneal treatment and implantation energy (VI.B).

VI.A. Excess Si or defect luminescence: Si versus Ne implants in SiO_2.

Figure 7(a) shows two room temperature PL spectra taken from a SiO_2 film implanted with $5 \cdot 10^{16}$ Si/cm^2 at 175 keV, before and after annealing. The spectrum from the as-implanted film shows a broad luminescence band with a maximum at 0.70 μm. After annealing at 700 °C for 40 minutes the spectrum peaks at a slightly longer wavelength (0.72 μm) and the PL signal decreased substantially.

Figure 7(b) shows the room temperature PL spectra taken from SiO_2 films implanted with $5 \cdot 10^{16}$ Ne/cm^2 at 175 keV before and after annealing. The as-implanted spectrum shows a broad feature around 0.66 μm. After giving this sample the same anneal treatment that was employed to the Si implanted sample (700 °C for 40 minutes), a completely flat PL spectrum of very low intensity results.

There are two possible explanations for the observed photoluminescence and the red-shift upon annealing in the Si implanted SiO_2 films. It may be that 1.) the photoluminescence is due to quantum confinement in Si crystallites that have already formed in the as-implanted sample. The mobility required for the nucleation and growth of these crystallites may have been supplied by the ion beam itself. Indeed, in-situ stress measurements have shown that the effective viscosity of SiO_2 during ion irradiation can be reduced by 6 orders of magnitude compared to the thermal value [19]. In a subsequent anneal treatment the average crystallite size would then increase as large crystallites grow at the expense of small ones (Ostwald

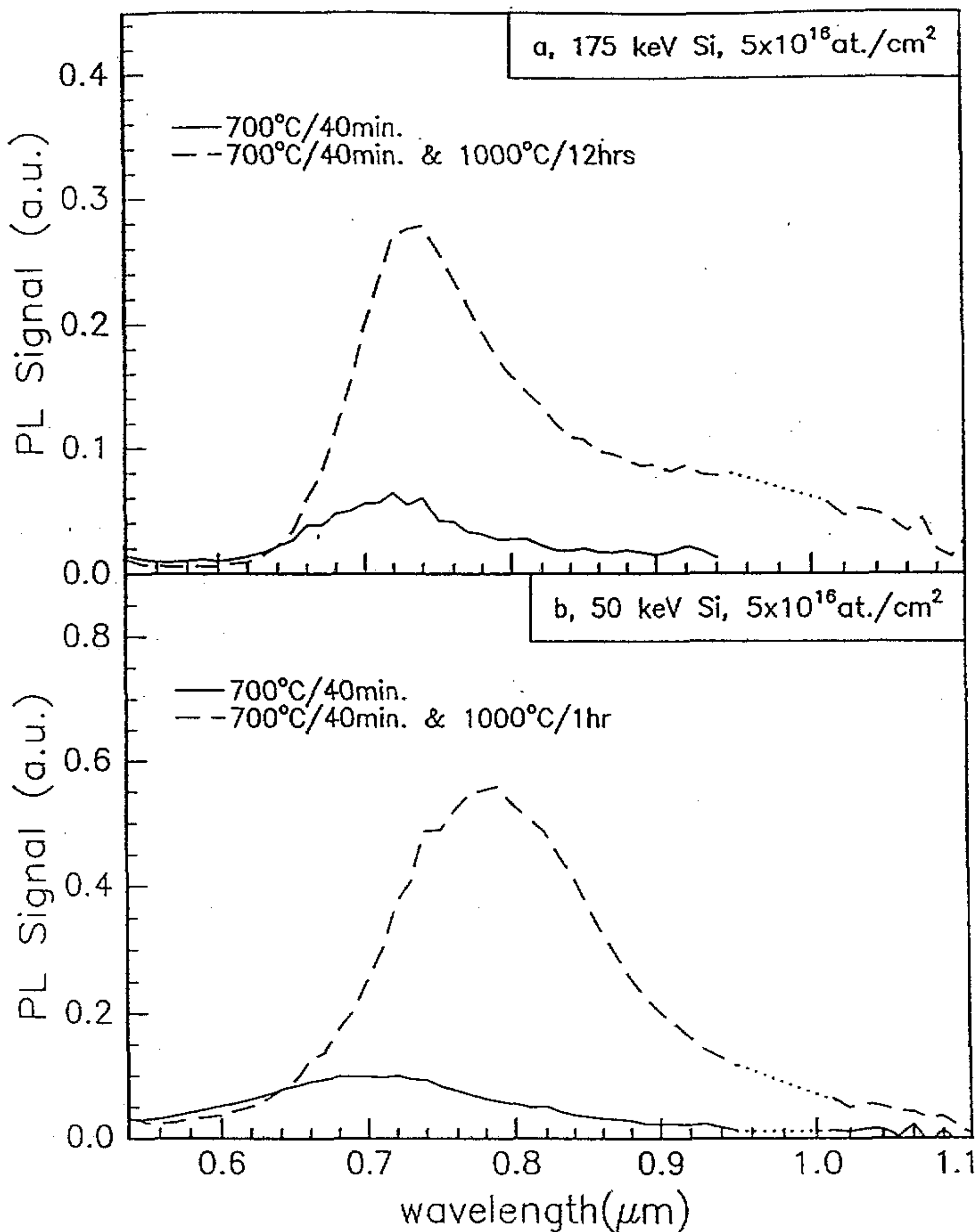

FIG.8 (a) Room temperature photoluminescence spectra for the SiO_2 film implanted with $5{\cdot}10^{16}$ Si/cm^2 at 175 keV, for two anneal treatments: 700 °C for 40 minutes or 700 °C for 40 minutes followed by 1000 °C for 12 hours. The second order reflection from the Ar-laser light (488 nm) off the grating was cut out of the spectrum and replaced by an interpolation of the data (dotted line).

(b) Same as (a) but know for an implant energy of 50 keV.

ripening). According to Fig.1, this would give rise to a red-shift of the PL signal.

Another explanation would be 2.) that the luminescence is related to the damage induced by the ion beam. It is well known that ion implantation produces changes in the structural and electronic properties of insulators, resulting in the formation of luminescence centers [18]. Indeed, this is seen in Fig. 7(b), where luminescence is observed from the Ne-implanted sample. As Ne is chemically inert, the luminescence is attributed to damage produced by the ion beam. The disappearance of the PL peak upon annealing is thus attributed to the annealing of damage. Indeed, previous work has shown that most of the damage created by the ion beam anneals in a broad stage from 300 °C to temperatures comparable to that used for the initial oxide growth (1000 °C) [20].

Comparing the Ne and Si data we conclude that the spectrum for the unannealed Si-implanted sample is (partly) due to beam induced effects. As these defects disappear upon annealing at 700 °C, we conclude that the luminescence observed from the annealed Si sample has to be attributed to the incorporation of excess Si.

VI.B. PL versus anneal temperature and implantation energy.

Figure 8(a) shows the PL spectra taken from a SiO_2 film implanted with $5 \cdot 10^{16}$ Si/cm^2 at 175 keV, for two anneal treatments. The spectrum taken from the sample after annealing at 700 °C for 40 minutes shows a broad, fairly symmetric band with a maximum at 0.72 μm. After an additional anneal at 1000 °C for 12 hours the spectrum shows an asymmetric luminescence peak with a tail towards the long wavelength side. The PL signal at the peak position has increased by a factor of about 4.5.

The spectra shown in Fig. 8(b) are taken from SiO_2 films that were implanted with the same dose ($5 \cdot 10^{16}$ Si/cm^2) as before but at an energy of 50 keV. The spectrum for the sample annealed at 700 °C for 40 minutes shows a broad feature at about 0.70 μm. The spectrum taken from the sample that received an additional anneal at 1000 °C for 1 hour shows a substantially red-shifted peak (maximum at about 0.78 μm) with a significantly higher PL signal. The increased contribution in the spectra at the long wavelength side, as well as the red-shift upon annealing, can be explained by the fact that Si clusters have formed after annealing at 700 °C. The average cluster size then increases upon annealing at 1000 °C. Further evidence that the luminescence indeed originates from Si clusters comes from a

comparison of the 175 keV and 50 keV implants. It can be noticed that the red-shift upon annealing at 1000 °C is much more pronounced for the 50 keV implanted sample. This can be explained by comparing the concentration depth profiles of both implants. Compared to a 175 keV implant, a 50 keV implant results in a smaller FWHM of the concentration depth profile and thus a higher peak concentration. As a consequence, nucleation and growth processes happen on shorter timescales. Si crystallites in the 50 keV implanted sample are thus expected to grow faster than those in the 175 keV implanted sample. Indeed, in Fig.8 a larger red-shift of the peak position is observed for the 50 keV implant than for the 175 keV implant.

For both implantation energies the overall PL signal increases upon annealing at 1000 °C. This is attributed to the annealing of defects in the Si crystallites themselves and at the Si/SiO_2 interface. Such defects may cause non-radiative recombination of carriers generated in the Si grains, thereby reducing the PL intensity.

It is interesting to note that the nucleation temperature of 700 °C is much lower than that observed for the SIPOS samples (1000 °C). This may lend further support for the idea that the mobility required for the nucleation and growth of small Si (subcritical) crystallites can be supplied by the ion beam itself. However, the higher temperature for SIPOS may also be attributed to the high O concentration.

Using the data in Figs 7 and 8 and the calculations in Fig. 1, we can now estimate that the typical cluster size is roughly 4 nm. It would be desirable to convert the PL spectra in Figs 7 and 8 into cluster-size distributions. In order to do this, corrections need to be made for the difference in absorption coefficients and radiative as well as non-radiative decay components for each cluster size. As all these parameters are unknown at this stage, it is not possible to determine the distribution over cluster sizes.

A final point worth noting is that, in contrast to porous Si [21], none of the annealed Si-implanted SiO_2 films showed luminescence in the spectral region below 0.60 μm. According to Fig. 1(a) this would mean that there are no Si crystallites smaller than 3.0 nm. This result is consistent with suggestions that the smallest (thermodynamically stable) size of Si precipitates in SiO_2 is about 2.5 nm [8,22]. This would imply that, unless other ways are invented to reduce this minimum size, the cluster luminescence wavelength will always be larger than ~ 500 nm.

VI.C PL spectroscopy on SIPOS

In the spectral range of 0.5 μm to 1.1 μm no luminescence was observed from the SIPOS films. This is an intriguing observation as the Si cluster volume fraction in this material is very large, and Raman spectroscopy has identified the presence of nm sized clusters (section V). Apparently at a Si concentration of 52 at.% the clusters are so close that coupling among the clusters makes effective quantum confinement of charge carriers impossible.

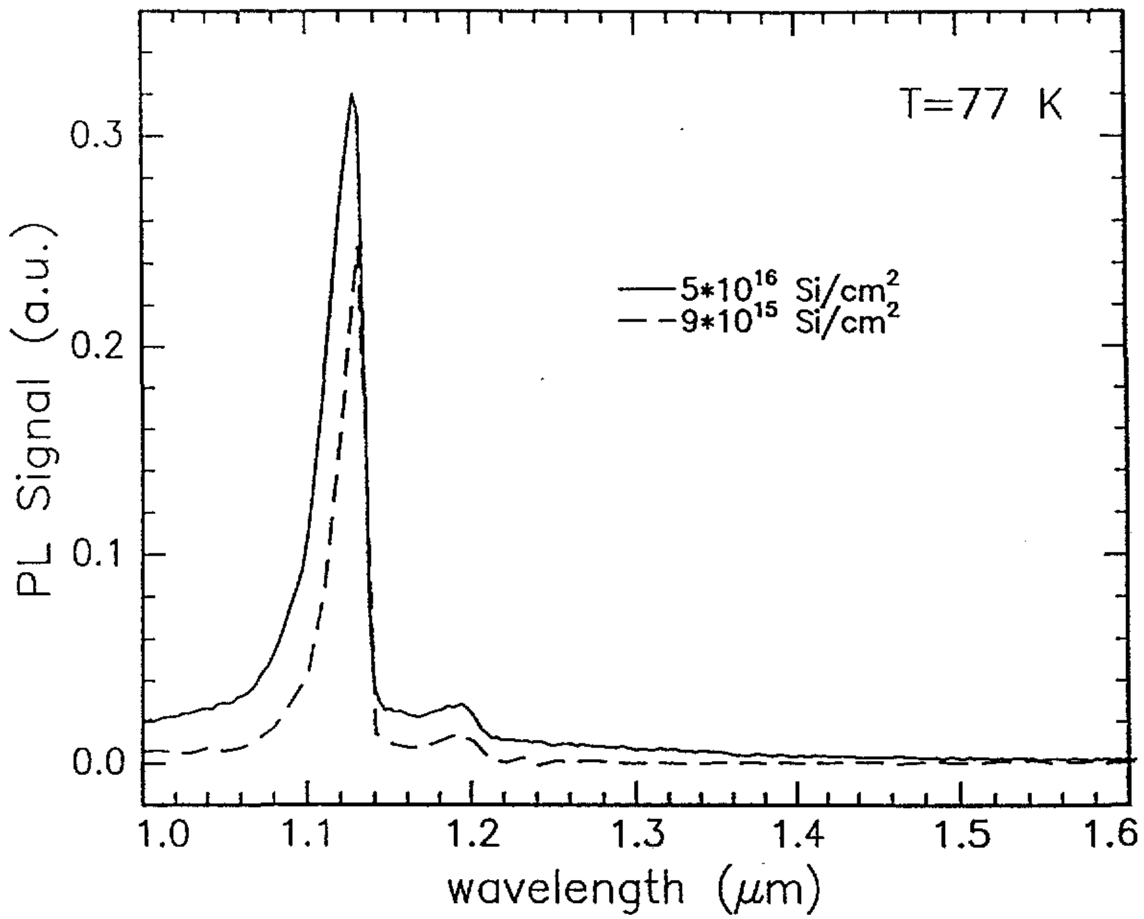

FIG.9. PL spectra taken at 77 K for the SiO_2 film implanted at 175 keV with either $9 \cdot 10^{15}$ Si/cm^2 or $5 \cdot 10^{16}$ Si/cm^2, after annealing at 700 °C for 40 minutes and 1000 °C for 12 hours.

VII. PHOTOLUMINESCENCE SPECTROSCOPY (1.0-1.6 μm) OF Si IMPLANTED SiO_2 FILMS

While much research activity has been devoted to the optical characterization of Si nano-crystals in the visible part of the spectrum, relatively little attention has been paid to the infra-red part. Recently Koch et al. [23] proposed that infra-red luminescence can originate from electronic states localized on the crystallite surface. We have investigated this possibility for the Si implanted SiO_2 films.

Figure 9 shows two PL spectra taken at 77 K from a SiO_2 film implanted at 175 keV with either $9{\cdot}10^{15}$ Si/cm^2 or $5{\cdot}10^{16}$ Si/cm^2 and after annealing at 700 °C for 40 minutes and 1000 °C for 12 hours. The features at 1.13 μm and 1.19 μm are attributed to phonon-assisted band-to-band recombination and exciton related recombination in the underlying Si substrate. For fluences up to $9{\cdot}10^{15}$ Si/cm^2 the spectrum shows a flat background signal of very low intensity. However, for a fluence of $5{\cdot}10^{16}$ Si/cm^2 the peaks due to the Si substrate are sitting on top of a very broad band. This band cannot originate from luminescence centra in the SiO_2 created by the ion beam, since they would have annealed out at 1000 °C for 12 hours [20]. Moreover, as a fluence of $9{\cdot}10^{15}$ Si/cm^2 is sufficient to damage SiO_2 to the saturation level, the IR tail should also have been observed for this implant. We attribute this band to transitions related to electronic states at the Si nano-crystallite/SiO_2 interface or in the Si clusters. It can thus be concluded that the quantum efficiency for band-to-band recombination in the Si nano-crystallites is less than 100 %.

VIII. CONCLUSIONS

Si crystallites with characteristic dimensions of ≤ 9 nm have successfully been grown by annealing LPCVD grown SIPOS films at 1200 °C for 5 minutes. Raman spectroscopy shows that an amorphous to crystalline transition takes place upon annealing at 1000 °C. The fact that no luminescence was observed from these films is attributed to the high Si concentration (52 at.%) which makes effective quantum confinement of charge carriers impossible.

After annealing at 700 °C for 40 minutes the Si implanted SiO_2 films show clear room temperature luminescence, attributed to band-to-band transitions in Si nano-crystals. A red-shift is observed upon annealing at 1000 °C, attributed to an increase in the average cluster size by Ostwald ripening. Comparing the 50 keV and 175 keV implants it is concluded that smaller clusters have formed when the Si supersaturation is less. Infrared luminescence observed in the range of 1.14 - 1.5 μm is attributed to electronic states localized at the Si/SiO_2 interface or in the Si nano-crystals. This indicates that the quantum efficiency for band-to-band recombination in the nano-crystals is less than 100 %.

IX. TECHNOLOGICAL ASSESSMENT.

Present-day Si-based technology has reached a high degree of sophistication. The possibility to take advantage of this vast knowledge to integrate optical and electronic components on a single substrate is a compelling one. Unfortunately, optoelectronics is still the domain of the expensive, and less developed III-V technology. To date, the role of Si has mainly been restricted to optically passive devices, for which the inefficient band-to-band recombination of Si is no problem.

A configuration having Si nano-crystals embedded in an SiO_2 matrix can, in principle, be used for the fabrication of optically active devices. For example, electroluminescence may be obtained from a metal-oxide-semiconductor (MOS)-type structure in which nano-crystallites are incorporated in the oxide film.

Furthermore, the increase of the refractive index which occurs when excess Si is incorporated into SiO_2 can be used to define optical waveguides in which the non-linear optical properties of Si clusters may be exploited. Because of the increased index, the optical modes would be centered at the Si doped region resulting in a good overlap between an excitation beam and the Si clusters. In planar optical waveguides high light intensities can be achieved due to the confinement of the optical modes, thereby enabling the study of Si clusters at much higher intensities than in the present studies. If Si with very high quantum efficiency can be obtained, the development of a Si cluster waveguide laser or amplifier may in principle be possible.

REFERENCES.

1. L.T. Canham, Appl. Phys. Lett. 57, 1046(1990)
2. J.P. Proot, C. Delerue and G. Allan, Appl. Phys. Lett. **61**, 1948(1992)
3. S. Furukawa and T. Miyasato, Phys. Rev. B. **38**, 5726(1988)
4. B. Delley and E.F. Stegmeier, Phys. rev. B. **47**, 1397(1993)
5. M.S. Brandt H.D. Fuchs M. Stutzmann, J Weber and M Cardona , Sol. State Commun. **81**, 307(1992)
6. S.M. George, M.B. Robinson and A.C. Dillon, Mat. Res. Soc. Symp. Proc. **298**, 289(1993)
7. S.L. Friedman, M.A. Marcus, D.A. Adler, Y.-H. Xie, T.D. Harris and P.H. Citrin, Mat. Res. Soc. Symp. Proc. **298**, 295(1993)
8. L.A. Nesbit, Appl. Phys. Lett. **46**, 38 (1985)
9. M. Catalano, M.J. Kim, R.W. Carpenter, K. Das Chowdhury and Joe Wong, J. Mater. Res. **8**, No. 11, 2893(1993)
10. T. Shimizu-Iwayama., J. Phys. Cond. Matter. **5**, 375(1993)
11. A. Polman, A.M. Vredenberg, W.H. Urbanus, P.J. van Deenen, H. Alberda, H. Krop, I. Attema, E. de Haas, H. Kersten, S. Doorn, J. Derks, J. ter Beek, S. Roorda, R. Schreutelkamp, J.G. Bannenberg and F.W. Saris, Nucl. Instr. and Meth. **B37/38**, 935(1989)
12. L.R. Doolittle, Nucl. Instr. and Meth. **B9**, 344(1985)
13. S. Hayashi, Y. Kanzawa M. Kataoka, T. Nagareda and K. Yamamoto, Z. Phys. **D26**, 144(1993)
14. J.C. Tsang, M.A. Tischler and R.T. Collins, Appl. Phys. Lett. **60**, (18), 2279(1992)
15. W.C. Sinke, T,Warabisako, M.Miyao, T, Tokuyama and S. Roorda, Appl. Surf. Sci, **36**, 460(1989)
16. I.H. Campbell and P.M. Fauchet, Solid State Comm. **58**, 739(1986)
17. J.A. Roth and G.L. Olson, Mater. Res. Soc. Symp. Proc. **74**, 319(1987)
18. P. Mazzoldi and G.W. Arnold, Ion beam modification of materials 2, Elsevier Science Publishers B.V. 1987.
19. C.A. Volkert and A.Polman, Mat. Res. Soc. Proc. **235**, 3(1992) and E.Snoeks A. Polman and C.A. Volkert, submitted to Appl. Phys. Lett.
20. E.P. EerNisse and C.B. Norris J. of Appl. Phys. **45**, (12), 5196(1974)
21. Y. Kanemitsu, T. Matsumoto, T.futagi and H. Mimura, Mat. Res. Soc. Symp. Proc. **298**, 205(1993)
22. S. Verprek, Z. Iqbal and F.-A. Sarott, Philos. Mag. B. **45**, 137(1982)
23. F. Koch, Mat. Res. Soc. Symp. Proc. **298**, 319(1993)

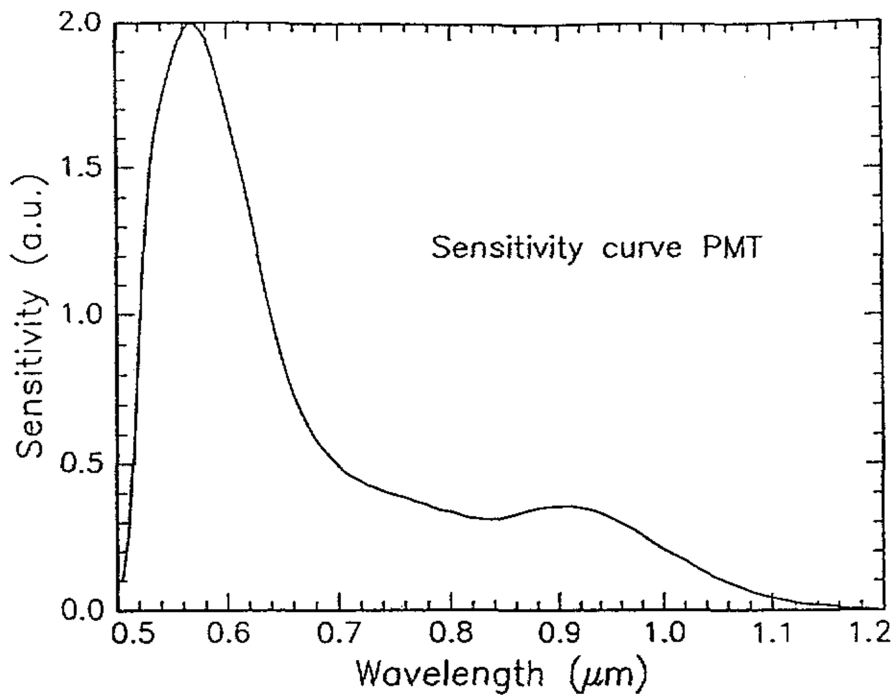

FIG.10. Sensitivity curve from the PMT measured with a calibrated W lamp. The maximum was normalized to 2. The corrected spectra are obtained by dividing the measured spectrum by the sensitivity curve.

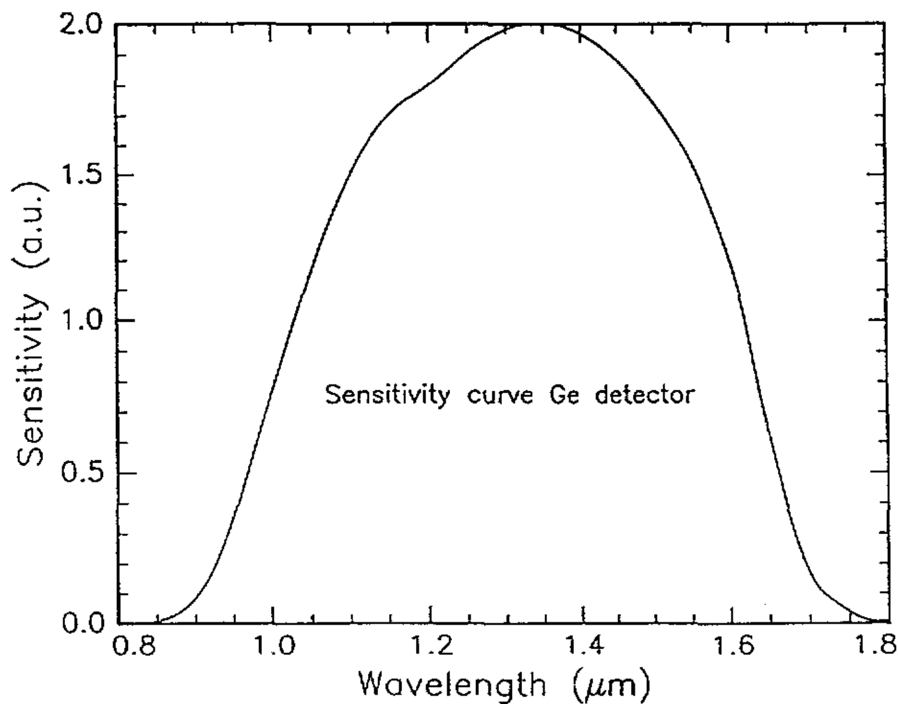

FIG.11. Sensitivity curve from the Ge detector measured with a W lamp. The maximum was normalized to 2.

APPENDIX I: Sensitivity curves from the PMT and Ge detector.

All the PL spectra presented were corrected for the sensitivity as a function of wavelength of the PMT and the Ge-detector. The sensitivities were determined using a calibrated W lamp (Philips, type W2KGV11I). First, PL spectra were taken from the W lamp using both the Ge detector and the PMT. These spectra were subsequently used for the calculation of a 'Sensitivity curve', which is defined as:

$$Sensitivity(\lambda)=\frac{Spectrum(\lambda)}{e_{bb}(\lambda)\times f_{corr.}(\lambda)}$$

where $e_{bb}(\lambda)$ is the photon density per unit of wavelength corresponding to a true black-body radiater:

$$e_{bb}(\lambda)\propto\frac{1}{\lambda^4}\times\frac{e^{-hc/kT}}{1-e^{hc/kT}}$$

and $f_{corr.}(\lambda)$ is a correction factor which compensates for the fact that the W lamp is not a true black-body radiater.

The sensitivity curves of the PMT and the Ge detector are shown respectively in Figs 10 and 11. The maxima of the curves was normalized to 2.00. Corrected spectra are obtained by dividing the measured spectra by the appropriate sensitivity curve.

ACKNOWLEDGEMENTS.

First of all, I would like to thank Prof. dr. F.W. Saris and Dr. A. Polman for making my stay at the AMOLF possible. I certainly enjoyed working in the ion implantation group and I am very grateful to all the group members for always being interested and willing to discuss my nm-sized problems. This work was performed in collaboration with Prof. H. Atwater at Caltech (Pasadena, USA), who also provided one of the samples in this study. Furthermore, Salvo Lombardo deserves a word of gratitude for making the SIPOS samples. I would also like to acknowledge Arjan Berntsen for collaborating with the Raman measurements. A final thanks goes to Prof. dr. M.J.A. de Voigt my supervisor at the Eindhoven University of Technology.